

Measurement of the signs of methyl ^{13}C chemical shift differences between interconverting ground and excited protein states by $R_{1\rho}$: an application to αB -crystallin

Andrew J. Baldwin · Lewis E. Kay

Received: 19 December 2011 / Accepted: 10 January 2012 / Published online: 5 April 2012
© Springer Science+Business Media B.V. 2012

Abstract Carr-Purcell-Meiboom-Gill relaxation dispersion (CPMG RD) NMR spectroscopy has emerged as a powerful tool for quantifying the kinetics and thermodynamics of millisecond time-scale exchange processes involving the interconversion between a visible ground state and one or more minor, sparsely populated invisible ‘excited’ conformational states. Recently it has also become possible to determine atomic resolution structural models of excited states using a wide array of CPMG RD approaches. Analysis of CPMG RD datasets provides the magnitudes of the chemical shift differences between the ground and excited states, $\Delta\omega$, but not the sign. In order to obtain detailed structural insights from, for example, excited state chemical shifts and residual dipolar coupling measurements, these signs are required. Here we present an NMR experiment for obtaining signs of ^{13}C chemical shift differences of $^{13}\text{CH}_3$ methyl groups using weak field off-resonance $R_{1\rho}$ relaxation measurements. The accuracy of the method is established by using an exchanging system where the invisible, excited state can be converted to the visible, ground state by altering sample conditions so that the signs of $\Delta\omega$ values obtained from the spin-lock

approach can be validated against those measured directly. Further, the spin-lock experiments are compared with the established H(S/M)QC approach for measuring signs of chemical shift differences and the relative strengths of each method are discussed. In the case of the 650 kDa human αB -crystallin complex where there are large transverse relaxation differences between ground and excited state spins the $R_{1\rho}$ method is shown to be superior to more ‘traditional’ experiments for sign determination.

Keywords Relaxation dispersion NMR · Invisible excited states · Protein conformational exchange · Spin-lock · Rotating frame relaxation

Introduction

Biological organisms rely on proteins to perform the majority of the chemical tasks required to sustain life. All the functions that proteins perform stem from the structures that they spontaneously adopt. Because these structures are stabilized by weak non-covalent interactions, at temperatures relevant to biology they are easily rearranged by thermal motion (Karplus and Kuriyan 2005). Proteins are consequently inherently dynamic molecules that are best understood as an ensemble of inter-converting conformers, rather than single, static structures (Alber et al. 1983; Lange et al. 2008; Lindorff-Larsen et al. 2005; Tolman et al. 1997). Biophysical studies of proteins are typically restricted to the set of conformers that make up the lowest energy basin. Higher energy conformational states however, are also sampled at room temperature. Such ‘excited’ states have been associated with important functional roles in biochemical processes including molecular recognition (Tang et al. 2006), ligand binding (Korzhev et al. 2009),

Electronic supplementary material The online version of this article (doi:10.1007/s10858-012-9617-6) contains supplementary material, which is available to authorized users.

A. J. Baldwin · L. E. Kay (✉)
Departments of Molecular Genetics, Biochemistry
and Chemistry, The University of Toronto, Toronto,
ON M5S 1A8, Canada
e-mail: kay@pound.med.utoronto.ca

L. E. Kay
Hospital for Sick Children, Program in Molecular Structure
and Function, 555 University Avenue, Toronto,
ON M5G 1X8, Canada

enzyme catalysis (Boehr et al. 2006; Fraser et al. 2009; Henzler-Wildman et al. 2007) and protein folding (Korzhev and Kay 2008). There is a clear need therefore to develop experimental tools to characterize these functionally important states in order to understand the mechanisms by which they interconvert with ground state conformers.

Recent advances in CPMG relaxation dispersion (CPMG RD) methodology (Hansen et al. 2008b; Palmer et al. 2001) enable studies of these otherwise ‘invisible’ excited states. Provided that exchange takes place with a highly populated conformation, that it is on the millisecond timescale and that the excited state is populated to at least 0.5%, CPMG RD experiments can be employed to reveal not only the thermodynamic and kinetic parameters that govern the exchange process, but also chemical shifts (Hansen et al. 2008b; Palmer et al. 2001), bond vector orientations (Vallurupalli et al. 2007), dihedral angles (Hansen et al. 2010) and motional parameters (Hansen et al. 2009) of the excited state. Taken together, it is now possible in some cases to determine structures of the excited state conformational ensemble (Bouvignies et al. 2011; Korzhnev et al. 2010; Vallurupalli et al. 2008b) at a level of detail that is starting to approach that with which the ground state can be characterized.

At present, the ‘toolkit’ of CPMG RD pulse sequences and labelling schemes allows the measurement of excited state backbone ^{15}N (Loria et al. 1999; Tollinger et al. 2001), $^1\text{H}^{\text{N}}$ (Ishima and Torchia 2003), $^{13}\text{C}^{\alpha}$ (Hansen et al. 2008c), $^1\text{H}^{\alpha}$ (Lundstrom et al. 2009), ^{13}CO (Ishima et al. 2004; Lundstrom et al. 2008) chemical shift differences, $^1\text{H}^{\text{N}}\text{-}^{15}\text{N}$, $^1\text{H}^{\alpha}\text{-}^{13}\text{C}^{\alpha}$, $^1\text{H}^{\text{N}}\text{-}^{13}\text{CO}$ residual dipolar couplings (Hansen et al. 2008a; Vallurupalli et al. 2007) and ^{13}CO residual chemical shift anisotropies (Vallurupalli et al. 2008a). More recently, experiments have been developed that extend these measurements to a number of side-chain positions, including $^{13}\text{C}^{\beta}$ (Lundstrom and Kay 2009), Asn/Gln ^{15}N (Mulder et al. 2001), Lys ^{15}N (Esadze et al. 2011), Asx/Glx ^{13}CO (Hansen and Kay 2011; Mulder and Akke 2003; Paquin et al. 2008) as well as methyl ^{13}C , ^1H (Baldwin et al. 2010; Lundstrom et al. 2007; Otten et al. 2010) sites and methyl $^1\text{H}\text{-}^{13}\text{C}$ RDCs (Baldwin et al. 2009).

CPMG relaxation dispersion experiments report the absolute values of the chemical shift differences ($|\Delta\nu|$ in Hz, $|\Delta\omega|$ in rad/sec, $|\Delta\sigma|$ in ppm). In order to exploit this information in structure calculations it is preferable to determine the sign of these shift differences and several experimental methods have been developed for this purpose. The first relies on the fact that chemical exchange will contribute differently to the evolution of single- and multiple-quantum coherences and that there is a static magnetic field strength dependence to the position of peaks (in ppm) in HSQC/HMQC spectra (Skrynnikov et al. 2002). It is possible therefore to obtain signs by measuring

the difference between peak positions in HSQC spectra acquired at two or more static magnetic field strengths or between correlations from HSQC/HMQC data sets (referred to in what follows as the H(S/M)QC approach). A second approach, the CEESY experiment (van Ingen et al. 2006), converts chemical shift differences into changes in cross-peak intensities that are subsequently quantified to extract the necessary sign information. Finally, a third approach, developed for ^{15}N , $^1\text{H}^{\alpha}$, $^1\text{H}^{\text{N}}$ and $^{13}\text{C}^{\alpha}$ nuclei (Auer et al. 2010, 2009) exploits the offset dependence of $R_{1\rho}$ rates that has been shown by Palmer and coworkers to be sensitive to the sign of $\Delta\sigma$ (Trott and Palmer 2002).

Herein, we extend our previous $R_{1\rho}$ methodology focusing on AX spin systems to the methyl group (AX_3) and present a ^{13}C $R_{1\rho}$ experiment for sign determination of methyl $\Delta\sigma_{\text{C}}$ values. The utility of this approach is demonstrated on a ligand–protein exchanging system that we have studied previously (Vallurupalli et al. 2007), comprised of a 17 residue peptide from the Ark1p protein (Haynes et al. 2007) and the Abp1p SH3 domain (Rath and Davidson 2000), where the chemical shift differences between ‘ground’ (free Abp1p SH3 domain) and ‘excited’ (Abp1p-Ark1p complex) states are known from previous studies. We show that accurate signs of $\Delta\sigma_{\text{C}}$ are obtained for shift differences in excess of approximately 0.1 ppm and provide a comparison between the $R_{1\rho}$ and H(S/M)QC approaches. An application of the methodology to a 650 kDa oligomeric ensemble of αB -crystallin (Horwitz 2009) is subsequently presented. This is a particularly challenging case because of large differences in intrinsic transverse relaxation rates of exchanging nuclei in the ground and excited states. It is shown that, in contrast to the H(S/M)QC method, the $R_{1\rho}$ experiment is less sensitive to these differences and that the signs of methyl $\Delta\sigma_{\text{C}}$ values could be obtained unequivocally for the two nuclei considered in αB -crystallin, unlike for the H(S/M)QC approach where the signs were ambiguous.

Materials and methods

Sample preparation

^{15}N , ^2H , Ile- $[\text{}^{13}\text{CH}_3\text{-}\delta 1]$, Leu-, Val- $[\text{}^{13}\text{CH}_3, \text{}^{12}\text{CD}_3]$ labelled Abp1p SH3 domain (Rath and Davidson 2000) and human αB -crystallin (Horwitz 2009) were prepared by protein over-expression in *E. coli*. (BL21(DE3)) grown in D_2O and M9 media with ^{12}C , ^2H glucose and ^{15}N ammonium chloride as carbon and nitrogen sources, respectively. Precursors α -ketobutyrate ($^{13}\text{CH}_3\text{CD}_2\text{COCO}_2\text{Na}$) and α -isovalerate ($^{13}\text{CH}_3(\text{CD}_3)\text{CDCOCO}_2\text{Na}$) were added one hour prior to induction of protein over-expression to obtain the appropriately labelled methyl groups (Goto et al. 1999;

Tugarinov and Kay 2004). Details of protein expression and purification for both the Abp1p SH3 domain and human α B-crystallin have been presented elsewhere (Baldwin et al. 2011a; Vallurupalli et al. 2007). ^2H Ark1p peptide (Haynes et al. 2007), which binds the SH3 domain, was generated as published previously (Vallurupalli et al. 2007). 7.5 mol percent peptide was added to a 200 μM Abp1p SH3 domain sample, as verified by ^{13}C relaxation dispersion experiments that quantify the fraction of bound protein. The SH3 domain—Ark1p complex was dissolved in buffer consisting of 50 mM sodium phosphate, 100 mM NaCl, 1 mM EDTA, 1 mM NaN_3 , 100% D_2O , pH = 7 (uncorrected). A second sample was prepared that was fully ligand bound and used to establish the accuracy of the excited state $R_{1\rho}$ experiment (see below). For human α B-crystallin the final protein concentration was 1 mM (monomer concentration) in a buffer consisting of 50 mM sodium phosphate, 1 mM EDTA, 1 mM NaN_3 , 100% D_2O pH = 5 (uncorrected). It is worth noting that sample deuteration is not a requirement for the experiments presented here although isolated ^{13}C methyl spins are important (i.e., carbon bonded to the methyl is not ^{13}C).

NMR spectroscopy and data analysis

In the case of the Abp1p SH3 domain-Ark1p peptide exchanging system 2D $R_{1\rho}$ data-sets were recorded with the scheme of Fig. 1, $T_{relax} = 40$ ms, focusing on one resonance at a time. In this manner the ^{13}C spin-lock carrier was placed at offsets of 0, $\pm|\Omega'|$ from the major (visible) correlation of interest and a separate spectrum recorded for each offset. It is important to emphasize that careful calibration of the resonance frequency of each of the sites is important (from which offsets = 0, $\pm|\Omega'|$ are established) especially if accurate signs of $\Delta\varpi_C$ values are to be obtained for small shift differences (see text). Because the positions of cross-peaks in HSQC spectra can have non-zero temperature coefficients we record a high resolution reference spectrum with $T_{relax} = 0$ and with ^1H CW decoupling applied immediately after the acquisition period (see Fig. 1c) for a duration equal to T_{relax} and use this reference to obtain peak positions. Values of $|\Omega'|$ and the strength of the spin-lock field, ω_1 , were optimized for individual $\Delta\varpi_C$ values (software can be downloaded from the Kay website) as described in Supporting Information using $k_{ex} = 160 \text{ s}^{-1}$ (the exchange rate), $p_E = 7.5\%$ (the population of the excited state) and $|\Delta\varpi_C|$ that were available from ^{13}C dispersion experiments that had been recorded previously (5°C). Datasets were recorded at a static magnetic field strength of 18.8T on a spectrometer with a room temperature probe. Each 2D plane was measured with acquisition times of (17, 64 ms) in (t_1 , t_2), 8 scans/FID and a relaxation delay between scans of 2 s for a

total measurement duration of 0.5 h/2D spectrum. Eleven resonances were considered, corresponding to those with $|\Delta\varpi_C| \geq 0.1$ ppm, leading to a net acquisition time of 16.5 h. Spectra were processed and analyzed with the program NMRPipe (Delaglio et al. 1995), signal intensities quantified by using the program FuDA (<http://pound.med.utoronto.ca/software>), and some data analysis performed with software that can be downloaded from the Kay website.

In the case of α B-crystallin signs of $\Delta\varpi_C$ for Ile159 δ 1 and Ile161 δ 1 were of interest. These were measured using the scheme of Fig. 1c (45°C, 18.8T), as described above, but here a series of 8 T_{relax} values ranging from 2 to 80 ms was chosen and $R_{1\rho}$ rates calculated from the intensity profiles of cross-peaks as a function of relaxation delay. Sample heating was maintained at a constant value irrespective of T_{relax} as described in the legend to Fig. 1. A total acquisition time of 7.2 h/residue was used.

Results and discussion

Experimental considerations

Consider a two-site exchanging system, $G \xrightleftharpoons[k_{EG}]{k_{GE}} E$, where the populations of the ground (G) and excited (E) states are in the limit $p_G \gg p_E$. In this case Trott and Palmer have shown that so long as $(R_2 - R_1)^2 \ll \Omega^2 + \omega_1^2$ the rotating frame longitudinal relaxation rate can be well approximated by (Trott and Palmer 2002),

$$R_{1\rho} = R_1 \cos^2 \theta + (R_2 + R_{ex}) \sin^2 \theta \quad (1)$$

where R_1 and R_2 are, respectively, the intrinsic longitudinal and transverse relaxation rates of the exchanging nucleus (assumed the same in both ground and excited states), R_{ex} is the contribution to transverse relaxation from the exchange process and θ is the angle that the spin-locked magnetization makes with respect to the z -axis. In Eq. [1] $\theta = \arctan(\omega_1/\Omega)$ where ω_1 (rad/s) is the strength of the spin-lock field and $\Omega = \omega_G - \omega_{SL}$, with ω_G , ω_{SL} the positions of the ground state resonance and the applied spin-lock, respectively. In addition, R_{ex} is given by

$$R_{ex} = \frac{p_E \Delta\omega^2 k_{ex}}{(\Omega + \Delta\omega)^2 + \omega_1^2 + k_{ex}^2} \quad (2)$$

where $k_{ex} = k_{GE} + k_{EG}$ and $\Delta\omega = \omega_E - \omega_G$ (rad s^{-1}). It is clear that a maximum in R_{ex} occurs when $\Omega = -\Delta\omega$, that is when the spin-lock field is placed at the resonance position of the excited state ($\omega_{SL} = \omega_E$). It is therefore possible to establish the sign of $\Delta\omega$ (or $\Delta\varpi$) by comparing $R_{1\rho}$ rates measured at $\Omega = \pm\Delta\omega$, since $R_{1\rho}(\Omega = -\Delta\omega) > R_{1\rho}(\Omega = \Delta\omega)$. Figure 1a, b illustrate this point. Shown schematically is a 1D ^{13}C spectrum highlighting the

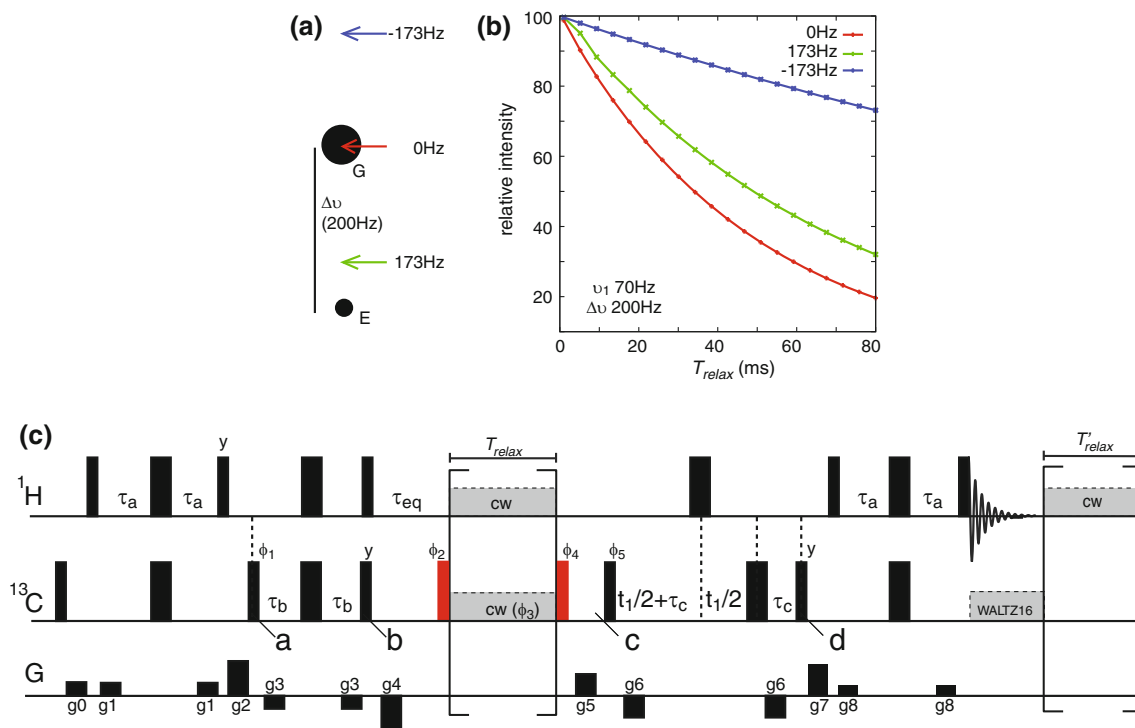


Fig. 1 **a** Schematic illustrating the approach for determination of the sign of ^{13}C methyl $\Delta\omega_C$ values based on off-resonance $R_{1\rho}$ measurements using weak spin lock fields. The positions of the ground (G) and excited (E) states for a single spin interconverting between a pair of states with $|\Delta\nu_C| \approx 200$ Hz, $p_E = 7.5\%$, $k_{ex} = 160$ s $^{-1}$ are indicated. The spin-lock field is placed on resonance for the major observable state (red arrow) and symmetrically $|\Omega'/(2\pi)|$ Hz upfield (blue) and downfield (green) from it. Optimal values for the positions of the spin-lock field were calculated as described in the text and in Supporting Information. **b** $R_{1\rho}$ decay curves 'measured' for each spin-lock position, establishing that the excited state resonance position lies downfield of the observable major state peak position. Values of $R_2 = 15$ s $^{-1}$ and $R_1 = 2.5$ s $^{-1}$ were used to generate the curves. **c** Pulse scheme for the determination of the sign of methyl $\Delta\omega_C$ values based on measurement of ^{13}C $R_{1\rho}$ rates. Pulses coloured black and red are applied at the highest possible power-levels along the x-axis unless indicated otherwise. The 'red' pulses are applied with a flip angle θ such that $\tan \theta = (\omega_1/\Omega')$ immediately prior to the application of the ^{13}C spin-lock CW field of strength ν_1 Hz. During this time a ^1H CW field is applied with a field of 10–15 kHz. ^{13}C decoupling during acquisition is achieved using a 2 kHz WALTZ-16 field (Shaka et al. 1983). The ^1H and ^{13}C carriers are initially placed on

the methyl resonance of interest; during the ^{13}C spin-lock period the carrier either remains 'on-resonance' or is moved $\pm|\Omega'|$ from the major state correlation. Immediately prior to point c the ^{13}C and ^1H carriers are placed in the center of the methyl region and on water, respectively. The durations τ_a , τ_b and τ_c are set to $\approx 1/(4J_{HC})$ (1.8 ms), 1.217 and 0.784 ms, respectively as described in the text. The delay $\tau_{eq} \approx 2-3/k_{ex}$ allows equilibration of magnetization prior to the application of the spin-lock. In order to ensure a constant level of sample heating in cases where a number of different T_{relax} values are recorded (i.e., heating independent of T_{relax}) a ^1H CW field of duration $T'_{relax} = T_{relax}(\text{max}) - T_{relax}$ where $T_{relax} \leq T_{relax}(\text{max})$ is applied after acquisition. The phase cycle for $\Omega' > 0$ (position of the spin-lock upfield of the major state resonance) is $\phi_1 = x, -x, \phi_2 = 2(y), 2(-y), \phi_3 = 2(x), 2(-x), \phi_4 = -\phi_2, \phi_5 = 4(x), 4(-x)$, and $\phi_{rec} = 2(x, -x), 2(-x, x)$. For $\Omega' < 0$, ϕ_2 and ϕ_4 are swapped. Note that the phases ϕ_2 and ϕ_4 may need to be inverted between different spectrometers (the cycle given is for Varian systems). Quadrature detection in F_1 is achieved via States-TPPI of ϕ_5 (Marion et al. 1989). Durations and strengths of the z-axis gradient pulses are (ms, G/cm), $g_0 = (1, 15)$, $g_1 = (0.5, 20)$, $g_2 = (0.8, 30)$, $g_3 = (0.6, -8)$, $g_4 = (1.0, -32)$, $g_5 = (0.7, 20)$, $g_6 = (0.3, -24)$, $g_7 = (0.4, 10)$ and $g_8 = (0.3, 12)$

positions of the ground and excited states for a single spin (Fig. 1a), $|\Delta\nu| \approx 200$ Hz. When the spin-lock field is positioned on resonance for the observed state (red arrow) a large $R_{1\rho}$ relaxation rate is observed (Fig. 1b, red). Placement of the spin-lock carrier downfield of the observed correlation by 173 Hz leads to an intermediate rate, green profile (173 is the 'optimized' value, see below). By contrast when the spin-lock is positioned upfield by 173 Hz, a low decay rate is obtained (blue). Since the 'green' decay curve corresponds to a larger $R_{1\rho}$ rate than the 'blue' profile the excited state resonance position must lie downfield of the ground state. In practice the position of

the observed major state correlation, ω_O , deviates slightly from ω_G due to exchange and for $p_G \gg p_E$ this deviation, ω_{ex} (rad/sec), can be calculated as (Skrynnikov et al. 2002)

$$\omega_{ex} = 2\pi\nu_{ex} = \frac{k_{EG}k_{GE}\Delta\omega}{(k_{EG} + \Delta R_2)^2 + (\Delta\omega)^2} \quad (3)$$

where $\Delta R_2 = R_2^E - R_2^G$ (assumed zero in most, but not all, of this work). In what follows we define $\Omega' = \omega_O - \omega_{SL}$ in direct analogy to Ω and therefore $\Omega = \Omega' - \omega_{ex}$. Only the magnitude of ν_{ex} is known in the absence of the sign of $\Delta\omega$ ($\Delta\omega$), as is the case here, so that while the position of the observed correlation can be obtained to a high level of

accuracy (see below) there are, of course, two possibilities for the position of the ground state corresponding to resonance frequencies of $\omega_O \pm |\omega_{ex}|$.

Figure 1c illustrates the pulse scheme for measurement of methyl ^{13}C $R_{1\rho}$ values. It is worth noting a priori that methyl ^{13}C longitudinal and transverse relaxation is non-exponential (Kay and Torchia 1991; Werbelow and Grant 1977) so that in general the decay of spin-locked ^{13}C magnetization cannot be characterized by a single time-constant, although we will not dwell on this here (see below). The flow of magnetization in the scheme of Fig. 1c can be summarized succinctly as,

$$H_Z \rightarrow 2C_{TR}H_Z \rightarrow C_Z \rightarrow SL(T_{relax}) \rightarrow 2C_{TR}H_Z(t_1) \rightarrow H_{TR}(t_2) \tag{4}$$

where t_1, t_2 denote acquisition times in the indirect and direct dimensions, respectively, A_j is the $j \in \{X, Y, Z\}$ component of A magnetization and SL, TR denote ‘spin-lock’ and ‘transverse magnetization’, respectively. The goal is to create in-phase carbon magnetization that can then be spin-locked so that ‘decay rates’ can be measured (Eq. [4], see below). Briefly, immediately after point *a* the magnetization of interest is given by $2C_YH_Z$. During the subsequent delay of duration $2\tau_b$ evolution due to the one-bond ^1H - ^{13}C scalar coupling (J_{HC}) leads to

$$2C_YH_Z \rightarrow -3 \sin\theta_b \cos^2\theta_b C_X + (\cos^3\theta_b - 2 \sin^2\theta_b \cos\theta_b) 2C_YH_Z + (\sin^3\theta_b - 2 \sin\theta_b \cos^2\theta_b) \sum_{i,j:i \neq j} 4C_XH_Z^iH_Z^j - (3 \sin^2\theta_b \cos\theta_b) 8C_YH_Z^1H_Z^2H_Z^3 \tag{5}$$

where $\theta_b = 2\pi J_{HC}\tau_b$ and the superscripts above each H_Z denote the proton from which the magnetization originates (where there are no superscripts H_Z refers to the sum over all three protons).

Magnetization denoted by terms proportional to H_Z or $H_Z^1H_Z^2H_Z^3$ is removed by the action of the ensuing gradient g_4 , while $4C_XH_Z^iH_Z^j$ is eliminated by setting the trigonometric term $(\sin^3\theta_b - 2 \sin\theta_b \cos^2\theta_b)$ to zero so that $\theta_b = \arccos(3^{-0.5})$; any residual doubly anti-phase magnetization that is not removed by this setting of θ_b is in part purged by application of the 90° ^1H pulse at point *b*. The remaining magnetization, C_Z , is rotated onto the spin-lock axis by a pulse of flip angle θ where $\theta = \arctan(\omega_1/\Omega')$, allowed to evolve for a time T_{relax} , and subsequently returned to the z axis by a $-\theta$ pulse. Subsequently, ^{13}C chemical shift is recorded during the t_1 interval between points *c* and *d*, during which time anti-phase magnetization is created that can be subsequently transferred back to ^1H for observation. For optimum sensitivity the delay τ_C is set

$$\text{to } \frac{\arccos(\sqrt{2/3})}{2\pi J_{HC}}$$

As described above the decay of magnetization during the T_{relax} period is expected to be non-exponential, primarily resulting from ^1H - ^{13}C dipole–dipole cross-correlated spin relaxation interactions that lead to the interconversion of ^{13}C in-phase (C_X, C_Z) and doubly anti-phase ($4C_XH_Z^iH_Z^j, 4C_ZH_Z^iH_Z^j$) components (Skrynnikov et al. 2001; Werbelow and Grant 1977). Cross-correlation effects can be minimized, but not eliminated, by ensuring that at the start of the spin-lock relaxation period only in-phase ^{13}C magnetization is present, as is done in the present experiment. Recording a series of 2D spectra with different T_{relax} values for each methyl group of interest would be very time-consuming and, additionally, the relaxation time-course would in general be non-exponential. Therefore, we prefer to choose a single T_{relax} delay, corresponding to 50–60% signal decay, for recording three data sets corresponding to offsets from the observed major state peak = 0, $\pm|\Omega'|$ rad/s, where positive values correspond to downfield and the value of $|\Omega'|$ is optimized for the exchange parameters and the $|\Delta\varpi_C|$ under consideration, see below and Supporting Information). In this case cross-peak intensities, $I(T_{relax}, \pm|\Omega'|)$, rather than relaxation rates are compared, with $I(T_{relax}, +|\Omega'|) < I(T_{relax}, -|\Omega'|)$ ($I(T_{relax}, +|\Omega'|) > I(T_{relax}, -|\Omega'|)$) indicating that the excited state is downfield (upfield) of the major state correlation. The value of $I(T_{relax}, \Omega' = 0)$ is obtained as a ‘control’, since it is expected that $I(T_{relax}, \Omega' = 0) < I(T_{relax}, \pm|\Omega'|)$.

As a final note, it is of interest to compare the sensitivity of this experiment ($T_{relax} = 0$) relative to a standard HSQC pulse scheme. Significant sensitivity losses are anticipated since it is not possible to completely transfer H_Z to C_Z for an AX_3 spin-system (see Eq. [5]), nor is it then possible to subsequently transfer in-phase ^{13}C magnetization back to ^1H for detection with perfect efficiency. Neglecting relaxation, the relative sensitivity is given by

$$\frac{I_{R_{1\rho}}}{I_{HSQC}} = (3 \sin\theta_b \cos^2\theta_b) \sin\theta_c \cos^2\theta_c = 0.31, \tag{6}$$

($\theta_c = 2\pi J_{HC}\tau_c$) comparable to what would be expected for a $^{13}\text{CHD}_2$ moiety (i.e., a single proton) where complete transfer of in-phase/anti-phase magnetization is possible. Note that the sensitivity is approximately 10–15% better than is expected for a sequence in which magnetization originates on ^{13}C , assuming a complete ^1H - ^{13}C NOE build-up.

Cross-validation of the methodology

As described previously, addition of a small mole fraction of a 17 residue peptide from the Ark1p protein to the Abp1p SH3 domain generates an exchanging system, $\text{Free}('Visible, Ground') \leftrightarrow \text{Bound}('Invisible, Excited')$,

that interconverts on the millisecond time-scale and is therefore amenable to study by CPMG RD experiments (Vallurupalli et al. 2007). Parameters of the ‘excited state’ generated via such experiments can be ‘tested’ by recording spectra on a sample where the bound state is the dominant form in solution. Of importance in this particular application is that the signs of $\Delta\varpi_C$ values are known with certainty so that the efficacy of the $R_{1\rho}$ method described can be established rigorously. Here we have ‘prepared’ an exchanging system with $p_E = 7.5\%$, $k_{ex} = 160 \text{ s}^{-1}$, 5°C (see “Materials and methods”). Of the 19 methyl groups in the SH3 domain, Fig. 2a, 11 show appreciable ^{13}C relaxation dispersion from which $|\Delta\varpi_C|$ values ranging from 0.1 ppm (Ile26 δ 1) to 2.3 ppm (Leu49 δ 1) are obtained; these methyl groups have been used to validate the methodology.

Three 2D experiments were recorded for each of the 11 methyls considered with offsets $0, \pm|\Omega'|/(2\pi)$ Hz using the pulse scheme shown in Fig. 1c, $T_{relax} = 40 \text{ ms}$. The inset to Fig. 2a, shows an example where for Ile26 δ 1 spectra were acquired with the spin-lock carrier on resonance with the major state observed peak (red arrow), $|\Omega'|/(2\pi)$ Hz downfield (green) and $|\Omega'|/(2\pi)$ Hz upfield (blue) for ‘optimal’ values of ω_1 and $|\Omega'|$. These were generated on a per-residue basis using $\{|\Delta\varpi_C|, k_{ex}, p_E, R_2\}$ obtained from

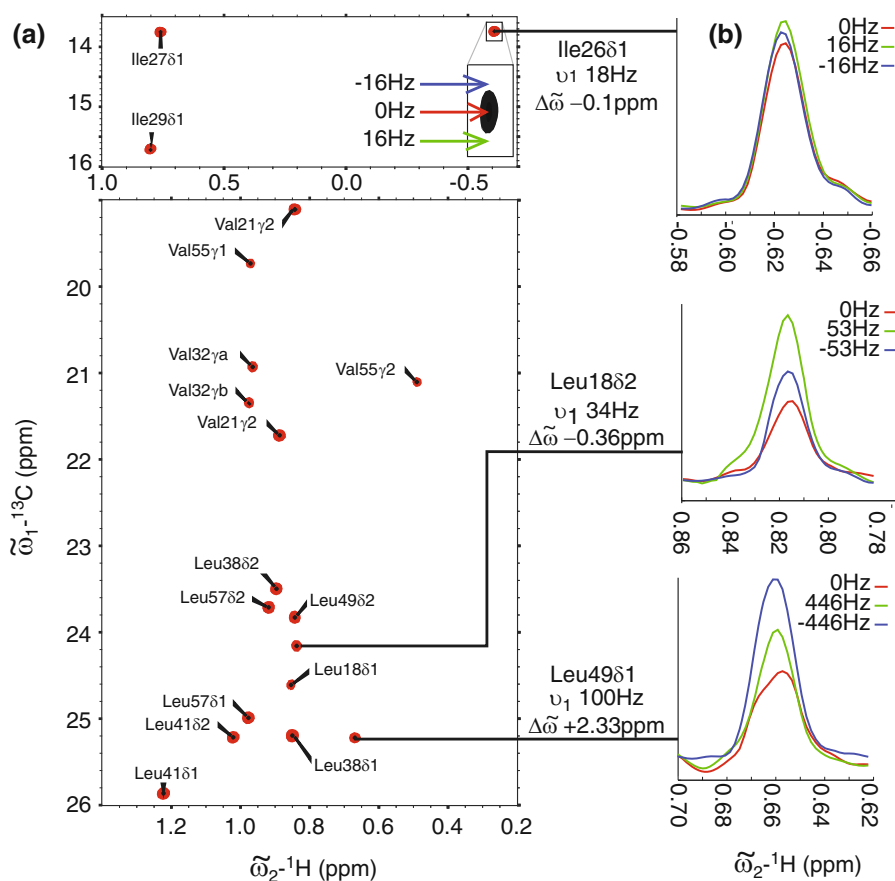
^{13}C methyl RD CPMG studies along with a value for R_1 of 2.5 s^{-1} by maximizing the difference

$$\Delta = |\exp(-R_{1\rho}(|\Omega'|)T_{relax}) - \exp(-R_{1\rho}(-|\Omega'|)T_{relax})| \quad (7)$$

using a procedure described in Supporting Information.

Figure 2b shows F_1 traces at the ^{13}C resonance positions for the Ile26 δ 1, Leu18 δ 2 and Leu49 δ 1 methyl groups in the Abp1p SH3 domain of the SH3-ligand exchanging system, colour-coded to indicate the position of the spin-lock carrier (see inset to Fig. 2a). For the first two methyls considered $I(T_{relax}, +|\Omega'|) > I(T_{relax}, -|\Omega'|)$ (compare blue and green peak intensities) so that the ^{13}C resonance position of the excited state lies upfield of the ground state chemical shift. By contrast, the situation is reversed for Leu49 δ 1, where the ^{13}C methyl chemical shift of the excited state is downfield of the methyl shift for the major conformer. The signs obtained for all 11 methyl groups considered are in agreement with those measured directly from spectra of unligated and fully bound SH3 domain samples. Of interest, the $R_{1\rho}$ method compares favourably with the previously developed H(S/M)QC approach where for 10 of the 11 methyl groups corresponding to $|\Delta\varpi_C| \geq 0.2 \text{ ppm}$ the signs are readily obtained from a comparison of peak positions in HSQC spectra recorded at

Fig. 2 **a** ^1H - ^{13}C spectrum of the Abp1p SH3 domain with 7.5% Ark1p peptide, 5°C , 18.8T acquired with the pulse scheme shown in Fig. 1c with $T_{relax} = 0$. Stereospecific assignments are available for all prochiral methyl groups with the exception of Val32; peaks for this residue are indicated by ‘a’ and ‘b’. **b** F_2 traces for selected residues showing differences in $I^\pm = I(T_{relax} = 40 \text{ ms}, \pm|\Omega'|)$ and $I^0 = I(T_{relax} = 40 \text{ ms}, 0)$ values from which the signs of $\Delta\varpi_C$ are obtained, as described in the text. Optimized values for $|\Omega'|$ and ν_1 are indicated



11.7 and 18.8T. For the remaining residue, Ile26 δ 1, $|\Delta\varpi_C| = 0.1$ ppm and the sign was available from an analysis of peak positions in HSQC/HMQC data sets since $|\Delta\varpi_H|$ is relatively large (0.05 ppm). In the case of the SH3 domain exchanging system both $R_{1\rho}$ and H(S/M)QC methods perform equally well (see below). Figure 3 shows a good correlation between calculated and experimental $\Lambda = \frac{I^+ - I^-}{I^+}$ values where $I^\pm = I(T_{relax}, \pm|\Omega'|)$ and $I^0 = I(T_{relax}, 0)$ for the 11 methyls in the SH3 domain for which $|\Delta\varpi_C| \geq 0.1$ ppm (red circles). Note further that the predicted and experimental signs of Λ are the same, an important criteria in validating the accuracy of the measurements.

In order to establish where the $R_{1\rho}$ approach would ‘fail’ we next considered three additional residues in the SH3 domain-peptide exchanging system, Leu57 δ 1, Leu41 δ 1 and Val21 γ 2. Essentially flat ^{13}C relaxation dispersion profiles were observed indicating that the $\Delta\varpi_C$ values must be very small. Indeed $\Delta\varpi_C = -0.06$ (Leu57), $+0.05$ (Leu41) and -0.04 (Val21) ppm, as established by direct comparison of ^1H - ^{13}C HSQC spectra of the SH3 domain, free and fully saturated with peptide. Calculated values of Λ were all close to zero, as expected for such small shift differences. Notably, near zero experimental values of Λ

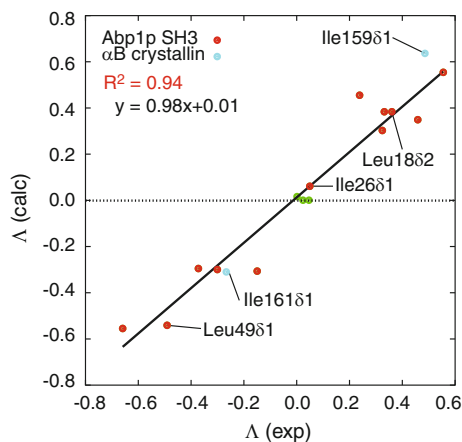


Fig. 3 Correlation between calculated (y-axis) and experimental (x-axis) $\Lambda = \frac{I^+ - I^-}{I^+}$ values where $I^\pm = I(T_{relax} = 40 \text{ ms}, \pm|\Omega'|)$ and $I^0 = I(T_{relax} = 40 \text{ ms}, 0)$ for the 11 residues in the SH3 domain for which $|\Delta\varpi_C| \geq 0.1$ ppm (red circles). Repeat values have been measured for a number of residues and are included as well. The value of the Pearson correlation coefficient squared, R^2 , is shown in the upper left hand corner (considering only the 11 SH3 domain methyl groups in red), along with the equation of the best fit line through the data (red). Λ ratios are also shown for Leu57 δ 1, Leu41 δ 1 and Val21 γ 2 for which essentially flat ^{13}C relaxation dispersion profiles were observed (green circles) as a control to ensure that small values are obtained. Also indicated are Λ ratios measured for Ile159 δ 1 and Ile161 δ 1 of αB -crystallin. Calculated values assumed $R_1 = 2.5 \text{ s}^{-1}$ and R_2 values as measured from CPMG relaxation dispersion profiles and in the case of αB -crystalline a value of $\Delta R_2 = 100 \text{ s}^{-1}$ was used

are also observed, providing further validation of the methodology. That this is the case is shown in Fig. 3, green circles.

Having shown that small values of $\Delta\varpi_C$ ‘produce’ small Λ values we next sought to establish a criterion that could be used in borderline cases to determine experimentally whether a sign is trustworthy. For example, from examination of the correlation plot of Fig. 3a high degree of confidence is obtained for the signs of all of the 11 methyls examined (red circles), with the exception of perhaps Ile26 δ 1, while signs for Leu57 δ 1, Leu41 δ 1 and Val21 γ 2 listed above cannot be obtained with any degree of certainty, as expected. Of course it is not surprising that when $\Delta\varpi_C$ is small ($< \approx 0.1$ ppm for the SH3—peptide system) it becomes difficult to extract sign information accurately and fortunately in these cases the signs are unimportant since $\omega_E \approx \omega_G$. However, it is constructive to consider how the experiment fails because, as we show below, this can be used as a diagnostic for the more ambiguous cases. Consider the case for Leu57 δ 1, illustrated schematically in Fig. 4a, where the excited state is 0.06 ppm (12 Hz at 18.8T) upfield from the ground state peak and where optimized ($\omega_1/(2\pi)$, $|\Omega'|/(2\pi)|$) values are (18, 16 Hz) (18.8T). Simulations (see Supporting Information) show that when the position of the observable state is identified accurately (1st column, red arrow corresponding to 0 Hz shift) $I(T_{relax}, |\Omega'|/(2\pi)|) = -16 \text{ Hz} < I(T_{relax}, |\Omega'|/(2\pi)|) = 16 \text{ Hz}$. In principle the correct sign can be determined in this case, at least in the limit of very high signal to noise so that the (very) small intensity difference can be quantified. The same scenario also holds where the position of the ‘on-resonance’ spin-lock is misset from the observable correlation by 0.5 Hz (2nd column), so that the spin-lock fields are applied at 15.5, 0.5 and -16.5 Hz. However, for a missetting of 1 Hz, as shown in the 3rd column of Fig. 4 $I(T_{relax}, |\Omega'|/(2\pi)|) = 15 \text{ Hz} < I(T_{relax}, |\Omega'|/(2\pi)|) = -17 \text{ Hz}$ and the wrong sign is obtained. This occurs because when the spin-lock field is placed at an offset of 15 Hz the contribution to $R_{1\rho}$ from the intrinsic R_2 of the ground state exceeds that due to exchange when the offset is placed at -17 Hz, slightly removed from the excited state.

For the SH3-peptide exchanging system considered here with $k_{ex} = 160 \text{ s}^{-1}$ and $p_E = 7.5\%$ (5°C) calculations show that a missetting of 1 Hz (as in Fig. 4a, 3rd column) can lead to errors in signs in cases for which $\Delta\varpi_C \leq 0.09$ ppm, as has been observed for Leu57 δ 1 (Fig. 4a). In contrast, for Ile26 δ 1 where $|\Delta\varpi_C| = 0.1$ ppm moving the spin-lock carrier positions ± 1 Hz from the calibrated ground state peak position did not lead to a change in the relative intensities of $I(T_{relax}, \pm|\Omega'|/(2\pi))$, providing confidence in its sign. The minimum $\Delta\varpi_C$ value for which signs ‘can be trusted’, $\Delta\varpi_C^{min}$, assuming a conservative error of 1 Hz in the estimated position of the

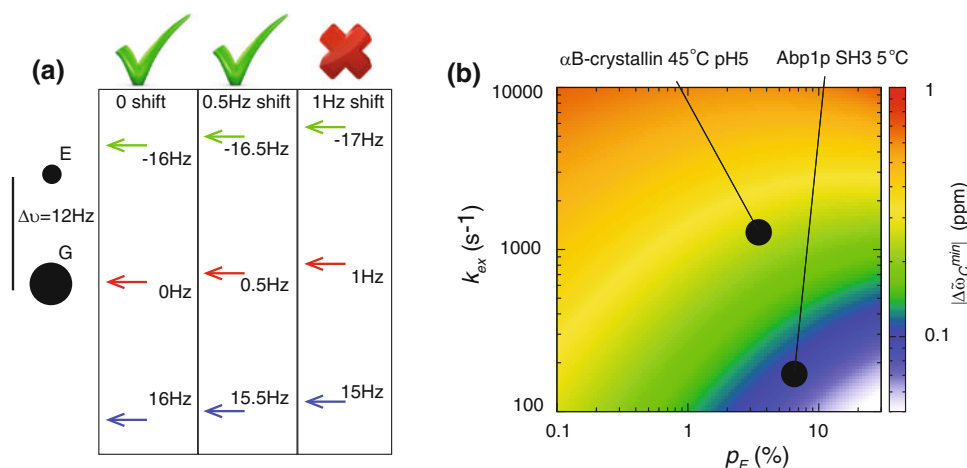


Fig. 4 a Schematic illustrating for Leu57 δ 1 from the SH3-Ark1p exchanging system (5°C) how a small missetting in the position of the spin-lock field can lead to errors in sign determination in certain pathological cases. In this example the excited state resonance position is 0.06 ppm (12 Hz at 18.8T) upfield from the major state peak, and optimized ($\omega_1/(2\pi)$, $|\Omega'/(2\pi)|$) values are (19, 16 Hz) (18.8T). Accurate sign values, based on the fact that $I(T_{relax}, |\Omega'/(2\pi)|) = -16$ Hz $<$ $I(T_{relax}, |\Omega/(2\pi)|) = 16$ Hz), are obtained when the spin-lock is correctly positioned or offset by an error of 0.5 Hz (columns 1 and 2). However,

for a missetting of 1 Hz, as shown in the 3rd column of Fig. 4 $I(T_{relax}, |\Omega/(2\pi)|) = 15$ Hz $<$ $I(T_{relax}, |\Omega'/(2\pi)|) = -17$ Hz) and the wrong sign is obtained. **b** The minimum $\Delta\sigma_C$ value for which signs ‘can be trusted’, $\Delta\sigma_C^{\min}$, is plotted as a function of p_E and k_{ex} . For $\Delta\sigma_C > \Delta\sigma_C^{\min}$ shifting the position of the spin-lock fields (0, $\pm|\Omega'/(2\pi)|$) by ± 1 Hz does not lead to changes in the signs of Λ . Shown on the plot are the (p_E , k_{ex}) values for Abp1p SH3-Ark1p and α B-crystallin exchanging systems with $\Delta\sigma_C^{\min} = 0.09$ ppm and $\Delta\sigma_C^{\min} = 0.25$ ppm, respectively

observed major state, ω_O , is plotted as a function of p_E and k_{ex} in Fig. 4b. In general $\Delta\sigma_C^{\min}$ decreases with p_E and increases with k_{ex} . An expression for $\Delta\sigma_C^{\min}$, accurate to within an error of approximately 5%, is given by

$$\Delta\sigma_C^{\min}(p_E, k_{ex}) = a \times (p_E)^b \times (k_{ex})^c \quad (8)$$

$$c = d \times (p_E)^e$$

with $a = 0.001697$, $b = -0.63187$, $d = 0.77034$ and $e = 0.191417$. We recommend estimating $\Delta\sigma_C^{\min}$ using the exchange parameters from dispersion experiments and Eq. [8] prior to measurement of signs, with $\Delta\sigma_C^{\min}$ used as a guide for selecting the set of methyl groups for further analysis. Once the $R_{1\rho}$ experiments have been recorded correlation plots of the sort indicated in Fig. 3 can be used to establish which residues are borderline and the ‘robustness’ of sign information verified by recording further experiments for these residues by shifting the position of the spin-lock fields (0, $\pm|\Omega'/(2\pi)|$) by ± 1 Hz and omitting any methyl groups for which signs of the experimentally determined Λ change.

Comparison of H(S/M)QC and $R_{1\rho}$ sign determination methods

As described above all 11 of the methyl groups in the Abp1p SH3 domain with $|\Delta\sigma_C| \geq 0.1$ ppm could be ‘signed’ correctly using both H(S/M)QC and $R_{1\rho}$ approaches. It is of interest to further explore the utility of the different methods over a wide range of exchange parameters. Figure 5 shows

results from simulations, including comparison of peak positions in (a) HSQC data sets recorded at 11.7 and 18.8T, (b, c) comparison of resonances in HSQC and HMQC spectra recorded at 11.7 T with $\Delta\sigma_H = 0.1$ ppm (b) or 0.5 ppm (c) and Δ values (Eq. [7]) from $R_{1\rho}$ measurements (d). Shown are contours of differences in peak positions, $\tilde{\delta}$, in the HS(M/Q)C experiments (a–c) or Δ in $R_{1\rho}$ measurements (d) as a function of k_{ex} and $|\Delta\sigma_C|$ for $p_E = 1\%$ (top row), 5% (middle row) and 10% (bottom row); we find that for ‘typical’ signal-to-noise values (moderately sized proteins with concentrations on the order of 1 mM) $\tilde{\delta}$ must be greater than 1–2 ppb, $\Delta > \approx 3$ –5% for the results to be significant experimentally.

Figure 5 illustrates the complementarity between the two H(S/M)QC based approaches (a–c), with the differences in peak positions in HSQC data sets recorded at 11.7 and 18.8 T more pronounced at higher k_{ex} and $|\Delta\sigma_C|$ values than from a comparison of HMQC and HSQC spectra. The $R_{1\rho}$ experiment performs particularly well for $\Delta\sigma_C$ values ≥ 0.1 –0.2 ppm, although so long as there is a large difference in 1 H chemical shifts between exchanging states, $\Delta\sigma_H$, (Fig. 5c) the HMQC/HSQC approach is preferred, at least for $k_{ex} \leq 1,000$ s⁻¹ and for low $\Delta\sigma_C$ values. Both $R_{1\rho}$ and HMQC/HSQC methods require data from only a single static magnetic field, however a significant advantage of the $R_{1\rho}$ experiment is that the result is independent of $\Delta\sigma_H$. Note also that there are certain regions in ($\Delta\sigma_C$, k_{ex}) space where differences in peak positions in HSQC/HMQC data sets produce erroneous signs; these are coloured black in

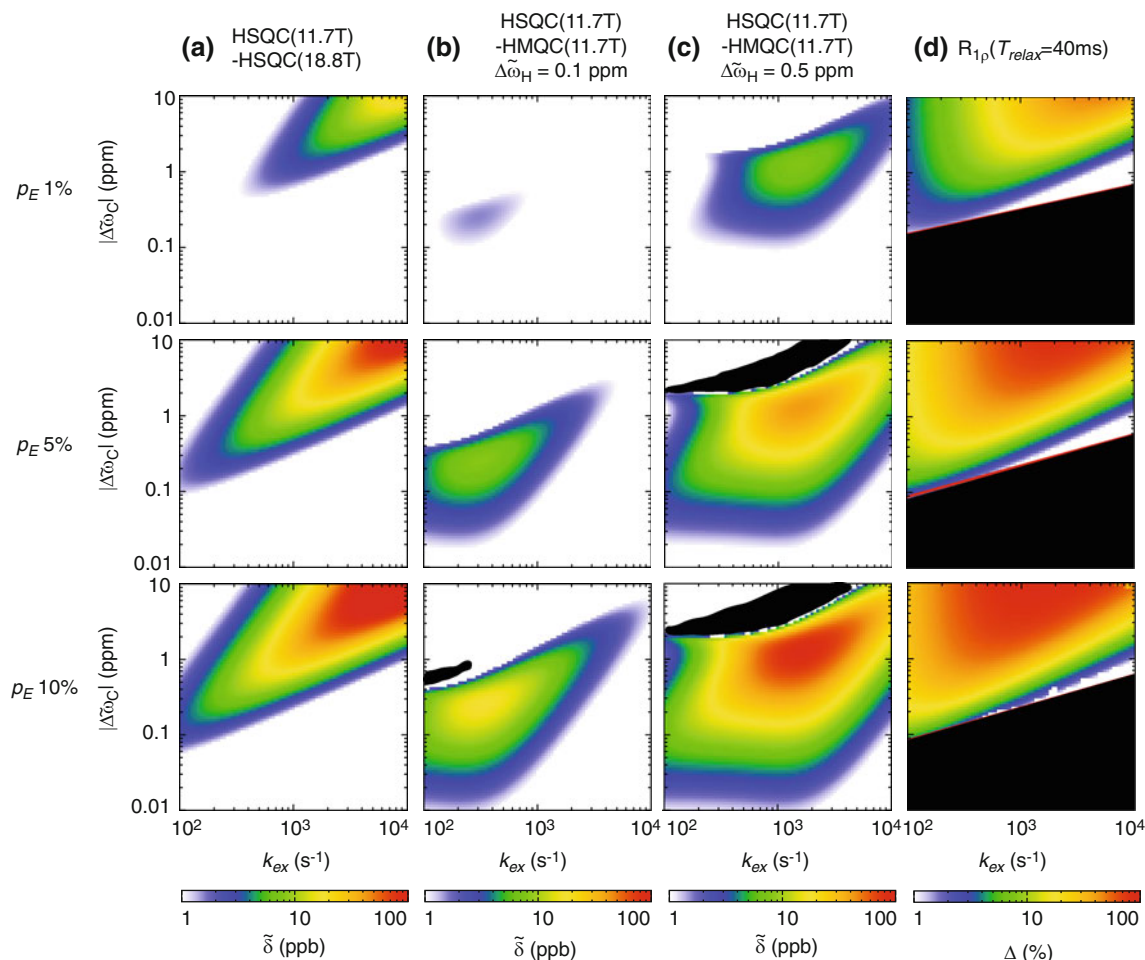


Fig. 5 Simulated contours of differences in peak positions, $\tilde{\delta}$, in HS(M/Q)C experiments (a–c) or Δ in $R_{1\rho}$ measurements (d) as a function of k_{ex} and $|\Delta\tilde{\omega}_C|$ for $p_E = 1\%$ (top row), 5% (middle row) and 10% (bottom row). In (a) HSQC data sets are ‘recorded’ at 11.7 and 18.8T, in (b, c) a comparison of resonance positions in HSQC and HMQC spectra at 11.7T with $\Delta\omega_H = 0.1$ ppm (b) or 0.5 ppm (c) is

presented and in (d) the static magnetic field is set to 18.8T. The regions in $(\Delta\tilde{\omega}_C, k_{ex})$ space where differences in peak positions in HSQC/HMQC data sets produce *erroneous signs* are coloured *black* in (b, c). In a similar manner the *black* region in panel (d) corresponds to $\Delta\tilde{\omega}_C$ values $\leq \Delta\tilde{\omega}_C^{min}$ where systematic errors in sign are obtained from $R_{1\rho}$ measurements. $\Delta R_2 = 0$ s⁻¹ is assumed in all simulations

Application to α B-crystallin

The human small heat shock protein α B-crystallin exists in a variety of exchanging oligomeric states centred on a mass of approximately 650 kDa (Baldwin et al. 2011b). We have previously established through a combined NMR and mass spectrometry analysis (Baldwin et al. 2011a) that the C-terminus of each monomer plays an important role in subunit exchange in this highly dynamic and heterogeneous assembly. Notably, ¹³C methyl RD CPMG studies focusing on the Ile159 δ 1 and Ile161 δ 1 C-terminal probes established a millisecond time-scale exchange process involving an interconversion between a ground and low

populated (invisible) state with $(k_{ex}, p_E) \approx (1240$ s⁻¹, 3.2%) at 45°C. In the ground state the Ile residues of interest are highly mobile, with methyl ¹³C δ 1 chemical shifts indicating a sampling of side-chain dihedral angle conformations as for a disordered peptide (Baldwin et al. 2011a). In contrast spin-state selective relaxation dispersion experiments establish that these side-chains become highly ordered in the excited state (unpublished data). Values of $|\Delta\tilde{\omega}_C|$ on the order of 1–2 ppm were fitted for each of the two sites, with the signs of the shift differences required for further structural insights.

Although differences in peak positions in HSQC spectra recorded at 11.7 and 18.8T were predicted to be in excess of 10 ppb, assuming $\Delta R_2 = 0$, only very small differences were observed that were either within or very close to the limits of experimental error (2 ppb or less). The discrepancy between predicted and expected $\tilde{\delta}$ values

presented and in (d) the static magnetic field is set to 18.8T. The regions in $(\Delta\tilde{\omega}_C, k_{ex})$ space where differences in peak positions in HSQC/HMQC data sets produce *erroneous signs* are coloured *black* in (b, c). In a similar manner the *black* region in panel (d) corresponds to $\Delta\tilde{\omega}_C$ values $\leq \Delta\tilde{\omega}_C^{min}$ where systematic errors in sign are obtained from $R_{1\rho}$ measurements. $\Delta R_2 = 0$ s⁻¹ is assumed in all simulations

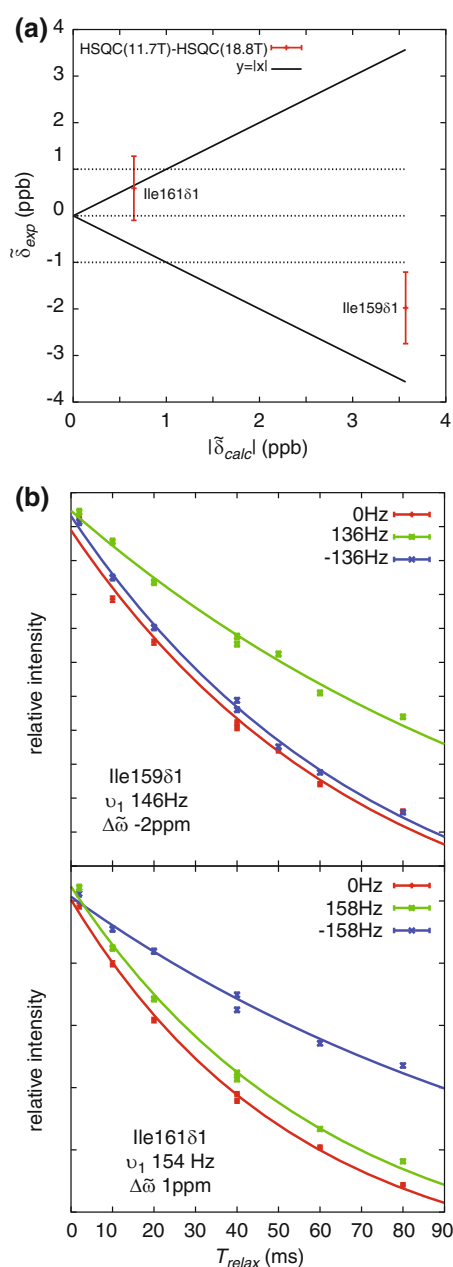


Fig. 6 An application to α B-crystallin. **a** Correlation between predicted and measured $\tilde{\delta}$ values assuming $\Delta R_2 = 100 \text{ s}^{-1}$. Values of $\tilde{\delta}$ are too small to obtain signs reliably. **b** $R_{1\rho}$ decay curves for Ile159 δ 1 (*top*) and Ile161 δ 1 (*bottom*) obtained using the experiment of Fig. 1c. Values of $(0, \pm|\Omega'|/2\pi)$ Hz and the strength of the spin-lock field are indicated for each methyl group. Unambiguous differences in $R_{1\rho}(+|\Omega'|)$ and $R_{1\rho}(-|\Omega'|)$ decay profiles were obtained so that signs of both $\Delta\varpi_C$ values could be ascertained

can be accounted for by the large ΔR_2 that is expected for a high molecular weight exchanging system involving probes localized to an unfolded region in the ground state and a well-organized folded conformation in the excited state (see Eq. [3]). Figure 6a shows the correlation between predicted and measured $\tilde{\delta}$ values assuming

$\Delta R_2 = 100 \text{ s}^{-1}$, consistent with recently recorded ^{13}C methyl spin-state selective RD CPMG profiles on this system.

$R_{1\rho}$ decay curves for Ile159 δ 1 (*top*) and Ile161 δ 1 (*bottom*) are shown in Fig. 6b. These were obtained using the experiment of Fig. 1c for spin-lock offset values of $(0, \pm|\Omega'|/2\pi)$ Hz which, along with the strength of the spin-lock field, have been individually optimized for each methyl group. In this case we have chosen to record the full decay curves (T_{relax} in the range 0–80 ms) since (i) only two peaks are considered and (ii) the C-terminus of the ground state is very dynamic so that near exponential $R_{1\rho}$ decay profiles are expected. Unambiguous differences in $R_{1\rho}(+|\Omega'|)$ and $R_{1\rho}(-|\Omega'|)$ decay profiles were obtained so that signs of both $\Delta\varpi_C$ values could be ascertained. While decreases in the efficacy of the HS(M/Q)C methodology with increasing ΔR_2 are expected from expressions derived by Skrynnikov et al. (2002) that take relaxation into account, of interest here is that $R_{1\rho}$ experiment appears to be more tolerant to such effects. Preliminary simulations, to be described in detail elsewhere, indicate that this is a general result.

In summary, an $R_{1\rho}$ pulse scheme has been presented for measurement of the signs of methyl $\Delta\varpi_C$ values in exchanging protein systems. The experiment is recorded in ‘2D mode’ minimizing problems with resolution associated with previously published $R_{1\rho}$ approaches based on the analysis of 1D spectra (Auer et al. 2010, 2009). Experimental time is minimized by recording only a small number of spectra for each methyl group of interest, corresponding to spin-lock fields at offsets of $(0, \pm|\Omega'|/2\pi)$ Hz from the observed correlation. The methodology has been demonstrated on a pair of systems including a protein–ligand exchanging complex where the results are rigorously cross-validated and a 650 kDa α B crystallin complex where previously published methods for sign determination failed. The $R_{1\rho}$ experiment thus provides an important addition to the NMR toolkit for studies of ‘excited’ conformational states.

Supplementary information

Formulae for the numerical evaluation of magnetization evolution due to an off-resonance spin-lock field and for the calculation of ω_{ex} are presented, along with a description of how optimized values of Ω' and ω_1 are obtained.

Software available

Python code for calculation of per-residue optimal values of $|\Omega'|$ and ω_1 based on input $\{|\Delta\varpi_C|, k_{ex}, p_E, R_2\}$ values from relaxation dispersion measurements. Code can be downloaded from the Kay website.

Acknowledgments AJB acknowledges the Canadian Institutes of Health Research (CIHR) for a postdoctoral fellowship. This work was supported by grants from the CIHR and the Natural Sciences and Engineering Research Council of Canada. LEK holds a Canada Research Chair in Biochemistry.

References

- Alber T, Gilbert WA, Ponzi DR, Petsko GA (1983) The role of mobility in the substrate binding and catalytic machinery of enzymes. *Ciba Found Symp* 93:4–24
- Auer R, Neudecker P, Muhandiram DR, Lundstrom P, Hansen DF, Konrat R, Kay LE (2009) Measuring the signs of $^1\text{H}(\alpha)$ chemical shift differences between ground and excited protein states by off-resonance spin-lock $R(\rho)$ NMR spectroscopy. *J Am Chem Soc* 131:10832–10833
- Auer R, Hansen DF, Neudecker P, Korzhnev DM, Muhandiram DR, Konrat R, Kay LE (2010) Measurement of signs of chemical shift differences between ground and excited protein states: a comparison between $\text{H}(\text{S}/\text{M})\text{QC}$ and $R(\rho)$ methods. *J Biomol NMR* 46:205–216
- Baldwin AJ, Hansen DF, Vallurupalli P, Kay LE (2009) Measurement of methyl axis orientations in invisible, excited states of proteins by relaxation dispersion NMR spectroscopy. *J Am Chem Soc* 131:11939–11948
- Baldwin AJ, Religa TL, Hansen DF, Bouvignies G, Kay LE (2010) $(^{13}\text{C})\text{CHD}(2)$ methyl group probes of millisecond time scale exchange in proteins by (^1H) relaxation dispersion: an application to proteasome gating residue dynamics. *J Am Chem Soc* 132:10992–10995
- Baldwin AJ, Hilton GR, Lioe H, Bagneris C, Benesch JL, Kay LE (2011a) Quaternary dynamics of αB -crystallin as a direct consequence of localised tertiary fluctuations in the C-terminus. *J Mol Biol* 413:310–320
- Baldwin AJ, Lioe H, Robinson CV, Kay LE, Benesch JL (2011b) αB -crystallin polydispersity is a consequence of unbiased quaternary dynamics. *J Mol Biol* 413:297–309
- Boehr DD, McElheny D, Dyson HJ, Wright PE (2006) The dynamic energy landscape of dihydrofolate reductase catalysis. *Science* 313:1638–1642
- Bouvignies G, Vallurupalli P, Hansen DF, Correia BE, Lange O, Bah A, Vernon RM, Dahlquist FW, Baker D, Kay LE (2011) Solution structure of a minor and transiently formed state of a T4 lysozyme mutant. *Nature* 477:111–114
- Delaglio F, Grzesiek S, Vuister GW, Zhu G, Pfeifer J, Bax A (1995) NMRPipe: a multidimensional spectral processing system based on UNIX pipes. *J Biomol NMR* 6:277–293
- Esadze A, Li DW, Wang T, Bruschweiler R, Iwahara J (2011) Dynamics of lysine side-chain amino groups in a protein studied by heteronuclear ^1H – ^{15}N NMR spectroscopy. *J Am Chem Soc* 133:909–919
- Fraser JS, Clarkson MW, Degnan SC, Erion R, Kern D, Alber T (2009) Hidden alternative structures of proline isomerase essential for catalysis. *Nature* 462:669–673
- Goto NK, Gardner KH, Mueller GA, Willis RC, Kay LE (1999) A robust and cost-effective method for the production of Val, Leu, Ile (d_1) methyl-protonated ^{15}N -, ^{13}C -, ^2H -labeled proteins. *J Biomol NMR* 13:369–374
- Hansen AL, Kay LE (2011) Quantifying millisecond time-scale exchange in proteins by CPMG relaxation dispersion NMR spectroscopy of side-chain carbonyl groups. *J Biomol NMR* 50:347–355
- Hansen DF, Vallurupalli P, Kay LE (2008a) Quantifying two-bond ^1HN – ^{13}CO and one-bond ^1Ha – ^{13}Ca dipolar couplings of invisible protein states by spin-state selective relaxation dispersion NMR spectroscopy. *J Am Chem Soc* 130:8397–8405
- Hansen DF, Vallurupalli P, Kay LE (2008b) Using relaxation dispersion NMR spectroscopy to determine structures of excited, invisible protein states. *J Biomol NMR* 41:113–120
- Hansen DF, Vallurupalli P, Lundstrom P, Neudecker P, Kay LE (2008c) Probing chemical shifts of invisible states of proteins with relaxation dispersion NMR spectroscopy: how well can we do? *J Am Chem Soc* 130:2667–2675
- Hansen DF, Vallurupalli P, Kay LE (2009) Measurement of methyl group motional parameters of invisible, excited protein states by NMR spectroscopy. *J Am Chem Soc* 131:12745–12754
- Hansen DF, Neudecker P, Vallurupalli P, Mulder FA, Kay LE (2010) Determination of Leu side-chain conformations in excited protein states by NMR relaxation dispersion. *J Am Chem Soc* 132:42–43
- Haynes J, Garcia B, Stollar EJ, Rath A, Andrews BJ, Davidson AR (2007) The biologically relevant targets and binding affinity requirements for the function of the yeast actin-binding protein I SRC-homology 3 domain vary with genetic context. *Genetics* 176:193–208
- Henzler-Wildman KA, Lei M, Thai V, Kerns SJ, Karplus M, Kern D (2007) A hierarchy of timescales in protein dynamics is linked to enzyme catalysis. *Nature* 450:913–916
- Horwitz J (2009) α crystallin: the quest for a homogeneous quaternary structure. *Exp Eye Res* 88:190–194
- Ishima R, Torchia D (2003) Extending the range of amide proton relaxation dispersion experiments in proteins using a constant-time relaxation-compensated CPMG approach. *J Biomol NMR* 25:243–248
- Ishima R, Baber J, Louis JM, Torchia DA (2004) Carbonyl carbon transverse relaxation dispersion measurements and ms-micros timescale motion in a protein hydrogen bond network. *J Biomol NMR* 29:187–198
- Karplus M, Kuriyan J (2005) Molecular dynamics and protein function. *Proc Natl Acad Sci USA* 102:6679–6685
- Kay LE, Torchia DA (1991) The effects of dipolar cross-correlation on ^{13}C methyl-carbon T_1 , T_2 and NOE measurements in macromolecules. *J Magn Reson* 95:536–547
- Korzhnev DM, Kay LE (2008) Probing invisible, low-populated states of protein molecules by relaxation dispersion NMR spectroscopy: an application to protein folding. *Acc Chem Res* 41:442–451
- Korzhnev DM, Bezsonova I, Lee S, Chalikian TV, Kay LE (2009) Alternate binding modes for a ubiquitin-SH3 domain interaction studied by NMR spectroscopy. *J Mol Biol* 386:391–405
- Korzhnev DM, Religa TL, Banachewicz W, Fersht AR, Kay LE (2010) A transient and low-populated protein-folding intermediate at atomic resolution. *Science* 329:1312–1316
- Lange OF, Lakomek NA, Fares C, Schroder GF, Walter KF, Becker S, Meiler J, Grubmuller H, Griesinger C, de Groot BL (2008) Recognition dynamics up to microseconds revealed from an RDC-derived ubiquitin ensemble in solution. *Science* 320:1471–1475
- Lindorff-Larsen K, Best RB, Depristo MA, Dobson CM, Vendruscolo M (2005) Simultaneous determination of protein structure and dynamics. *Nature* 433:128–132
- Loria JP, Rance M, Palmer AG (1999) A relaxation compensated CPMG sequence for characterizing chemical exchange. *J Am Chem Soc* 121:2331–2332
- Lundstrom P, Kay LE (2009) Measuring ^{13}C chemical shifts of invisible excited states in proteins by relaxation dispersion NMR spectroscopy. *J Biomol NMR* 44:139–155

- Lundstrom P, Vallurupalli P, Religa TL, Dahlquist FW, Kay LE (2007) A single-quantum methyl ^{13}C -relaxation dispersion experiment with improved sensitivity. *J Biomol NMR* 38:79–88
- Lundstrom P, Hansen DF, Kay LE (2008) Measurement of carbonyl chemical shifts of excited protein states by relaxation dispersion NMR spectroscopy: comparison between uniformly and selectively (^{13}C) labeled samples. *J Biomol NMR* 42:35–47
- Lundstrom P, Hansen DF, Vallurupalli P, Kay LE (2009) Accurate measurement of alpha proton chemical shifts of excited protein states by relaxation dispersion NMR spectroscopy. *J Am Chem Soc* 131:1915–1926
- Marion D, Ikura M, Tschudin R, Bax A (1989) Rapid recording of 2D NMR spectra without phase cycling. Application to the study of hydrogen exchange in proteins. *J Magn Reson* 85:393–399
- Mulder FA, Akke M (2003) Carbonyl ^{13}C transverse relaxation measurements to sample protein backbone dynamics. *Magn Reson Chem* 41:853–865
- Mulder FAA, Skrynnikov NR, Hon B, Dahlquist FW, Kay LE (2001) Measurement of slow timescale dynamics in protein sidechains by ^{15}N relaxation dispersion NMR spectroscopy: application to Asn and Gln residues in a cavity mutant of T4 lysozyme. *J Am Chem Soc* 123:967–975
- Otten R, Villali J, Kern D, Mulder FA (2010) Probing microsecond time scale dynamics in proteins by methyl (^1H) Carr-Purcell-Meiboom-Gill relaxation dispersion NMR measurements. Application to activation of the signaling protein NtrC(r). *J Am Chem Soc* 132:17004–17014
- Palmer AG, Kroenke CD, Loria JP (2001) NMR methods for quantifying microsecond-to-millisecond motions in biological macromolecules. *Methods Enzymol* 339:204–238
- Paquin R, Ferrage F, Mulder FA, Akke M, Bodenhausen G (2008) Multiple-timescale dynamics of side-chain carboxyl and carbonyl groups in proteins by ^{13}C nuclear spin relaxation. *J Am Chem Soc* 130:15805–15807
- Rath A, Davidson AR (2000) The design of a hyperstable mutant of the Abp1p SH3 domain by sequence alignment analysis. *Protein Sci* 9:2457–2469
- Shaka AJ, Keeler J, Frenkiel T, Freeman R (1983) An improved sequence for broadband decoupling: WALTZ-16. *J Magn Reson* 52:335–338
- Skrynnikov NR, Mulder FAA, Hon B, Dahlquist FW, Kay LE (2001) Probing slow time scale dynamics at methyl-containing side chains in proteins by relaxation dispersion NMR measurements: application to methionine residues in a cavity mutant of T4 lysozyme. *J Am Chem Soc* 123:4556–4566
- Skrynnikov NR, Dahlquist FW, Kay LE (2002) Reconstructing NMR spectra of “invisible” excited protein states using HSQC and HMQC experiments. *J Am Chem Soc* 124:12352–12360
- Tang C, Iwahara J, Clore GM (2006) Visualization of transient encounter complexes in protein-protein association. *Nature* 444:383–386
- Tollinger M, Skrynnikov NR, Mulder FAA, Forman-Kay JD, Kay LE (2001) Slow dynamics in folded and unfolded states of an SH3 domain. *J Am Chem Soc* 123:11341–11352
- Tolman JR, Flanagan JM, Kennedy MA, Prestegard JH (1997) NMR evidence for slow collective motions in cyanometmyoglobin. *Nat Struct Biol* 4:292–297
- Trott O, Palmer AG 3rd (2002) $R_{1\rho}$ relaxation outside of the fast-exchange limit. *J Magn Reson* 154:157–160
- Tugarinov V, Kay LE (2004) An isotope labeling strategy for methyl TROSY spectroscopy. *J Biomol NMR* 28:165–172
- Vallurupalli P, Hansen DF, Stollar EJ, Meirovitch E, Kay LE (2007) Measurement of bond vector orientations in invisible excited states of proteins. *Proc Natl Acad Sci USA* 104:18473–18477
- Vallurupalli P, Hansen DF, Kay LE (2008a) Probing structure in invisible protein states with anisotropic NMR chemical shifts. *J Am Chem Soc* 130:2734–2735
- Vallurupalli P, Hansen DF, Kay LE (2008b) Structures of invisible, excited protein states by relaxation dispersion NMR spectroscopy. *Proc Natl Acad Sci USA* 105:11766–11771
- van Ingen H, Vuister GW, Wijmenga S, Tessari M (2006) CEESY: characterizing the conformation of unobservable protein states. *J Am Chem Soc* 128:3856–3857
- Werbelow LG, Grant DM (1977) Intramolecular dipolar relaxation in multispin systems. *Adv Magn Reson* 9:189–299